Metallomics

Accepted Manuscript

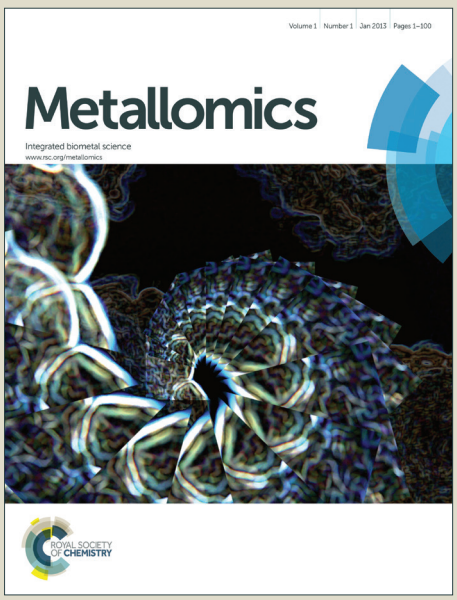

ROYAL SOCIETY OF CHEMISTRY

www.rsc.org/metallomics

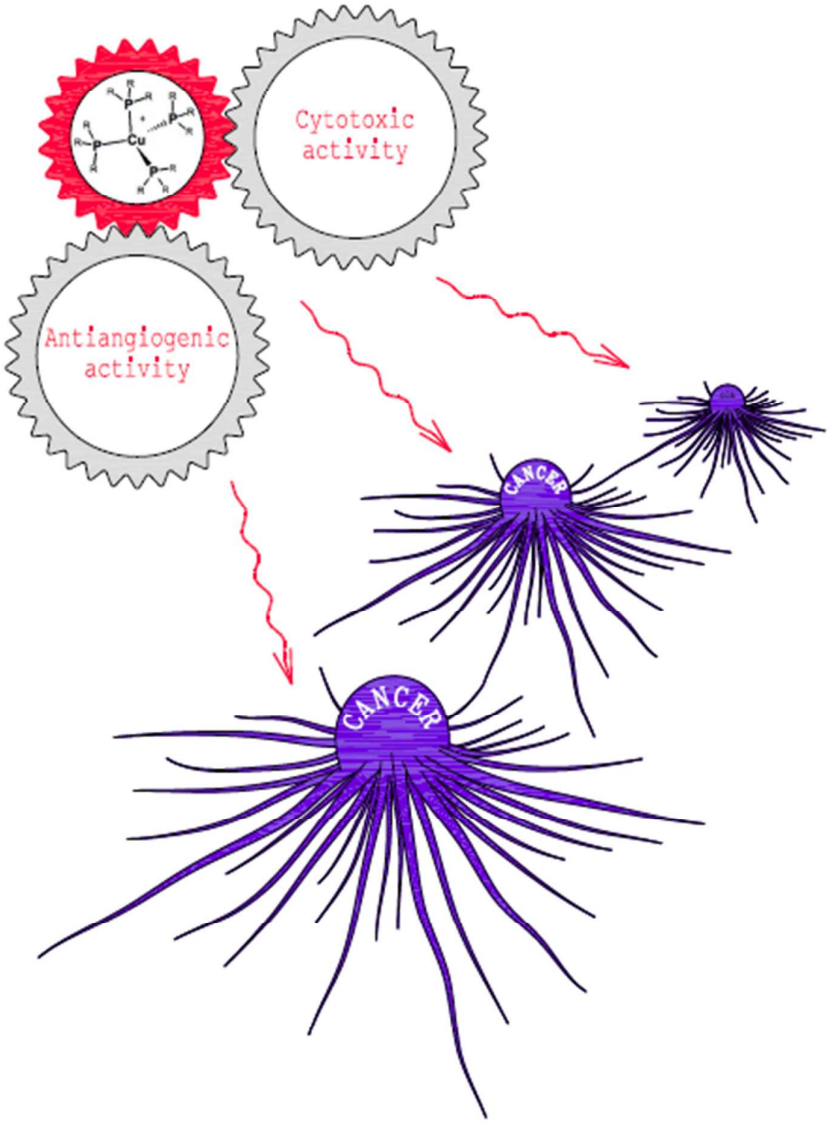

A series of homoleptic Phosphino Copper(I) Complexes inhibit cancer cell growth and angiogenesis in cultured cells and in animal models.

Metallomics

RSCPublishing

ARTICLE

Homoleptic Phosphino Copper(I) Complexes with in Vitro and in Vivo Dual Cytotoxic and Anti-angiogenic Activity

Cite this: DOI: 10.1039/xoxxoooooox

Received ooth January 2012,
Accepted ooth January 2012

DOI: 10.1039/xoxxoooooox

www.rsc.org/

V. Gandin,[a‡] A. Trenti,[a‡] M. Porchia,[b] F. Tisato,[b] M. Giorgetti,[c] I. Zanusso,[a] L. Trevisi[a] and C. Marzano[a]*

Homoleptic, tetrahedral Cu(I) complexes of the type $[Cu(P)_4]BF_4$ (**1-3**), where P are the phosphine ligands 1,3,5 –triaza-7-phosphaadamantane (PTA), 3,7-diacetyl-1,3,7-triaza-5-phosphabicyclo[3.3.1] nonane (DAPTA) and 2-thia-1,3,5-triaza-phosphoadamantane 2,2 dioxide (PTA-SO_2), have been prepared. The novel complexes $[Cu(DAPTA)_4]BF_4$ **2** and $[Cu(PTA\text{-}SO_2)_4]BF_4$ **3** have been fully characterized by means of spectroscopic methods, corroborated by XAS-EXAFS analysis on **2.** *In vitro* cell culture experiments revealed a significant antiproliferative activity for Cu(I) compounds against several human cancer cell lines derived from solid tumors with a preferential cell growth inhibition towards tumour than non-malignant cells. In vitro monitoring of migration and capillary-like tube formation of human umbilical vein endothelial cells (HUVEC) showed an anti-angiogenic effect of copper(I) complexes at sub-cytotoxic concentrations. *In vivo* studies on the antitumor efficacy and ability to inhibit angiogenesis confirmed the dual cytotoxic and anti-angiogenic property of Cu(I) derivatives.

Introduction

In the search for novel metal-based drugs useful for addressing anticancer therapy, recent findings have demonstrated that copper complexes represent good alternatives to platinum drugs.[1] Actually, copper species, besides possessing a broader spectrum of activity and a lower toxicity, are able to overcome inherited and/or acquired resistance to cisplatin. These features are consistent with the hypothesis that copper complexes possess mechanism(s) of action different from those shown by platinum drugs. Recently, numerous experimental evidences indicated that copper metabolism is severely altered in neoplastic diseases. In particular, elevated serum copper concentrations correlate well with tumour burden, progression, and recurrence in a variety of human cancers such as Hodgkin's lymphoma, sarcoma, cervix, prostate, liver, lung, brain and breast cancers.[2-4] Although the molecular mechanism underlying copper rise in malignant cells remains poorly understood, it looks partially explainable taking into consideration the role that copper plays in tumour angiogenesis, especially at the early stages.[5] Copper seems to take part in angiogenesis by stimulating proliferation and migration of human endothelial cells, and by acting as co-factor of several angiogenic factors, such as VEGF, bFGF, TNF-a, angiogenin and IL1.[6] The effect of copper on VEGF expression has been demonstrated and exploited in many cases when there is a need for rapid formation of micro vessels. For example, it has been reported that the use of copper sulphate determines a faster closure of the dermal wounds so that application of copper sulfate and VEGF has been proposed in regenerative medicine.[7] In a rather contrasting approach, copper depletion agents utilized to reduce copper content in angiogenic tissues related to cancer proliferation (referred to as 'copper chelation therapy') are currently tested in clinical phase II. However, very recent studies report that copper chelation therapy may produce, in certain cases, an angiogenesis enhancement.[8, 9] These contrasting evidences support the idea that processes underlying the role of copper in angiogenesis have not been completely clarified yet. Angiogenesis-driven or not, tumor tissues have proved to be avid of copper. This feature may turn tumor cells into targets for Cu-based drugs, whereas non-tumour cells may promote the elimination of excess Cu through homeostatic mechanisms.

Our research group has a long-time interest in designing phosphine copper(I) compounds as potential anticancer agents. Hydrophilic tertiary phosphines (P) have been used to obtain stable, water-soluble $[Cu(P)_4]^+$ species that proved to be easy to handle during in vitro tests and showed promising antiproliferative effects.[10, 11] In particular, the monocationic $[Cu(thp)_4][PF_6]$ complex (thp = tris-hydroxymethylphosphine) showed excellent in vitro antitumor activity against a wide range of solid tumors,[10] including platinum drug refractory/resistant tumors.[12] Moreover, $[Cu(thp)_4][PF_6]$ was much less cytotoxic against non-tumor cells than Pt(II) drugs with selectivity index (SI, the quotient of the average IC_{50} toward non-malignant cells divided by the average IC_{50} for the malignant cells) values about 35- and 10-fold higher than those calculated for cisplatin and oxaliplatin, respectively.[12]

Whereas for several years the search for anticancer drugs has been focused on the suppression of cancer cell growth, more recently it has been demonstrated that the inhibition of angiogenesis represents another promising antitumor strategy. Several 'accidental' angiogenesis inhibitors have been discovered among conventional cytotoxic chemotherapeutics.[13] The current interest in developing multiple anticancer functional drugs relies on the assumption that

these bioactive compounds may enhance anticancer potency by reducing the risk of systemic toxicity induced upon separate use of cytotoxic and antioangiogenic drugs.[14]

For some classes of gold(I,III) and ruthenium(II,III) complexes, a dual cytotoxic and antiangiogenic activity has already been described.[15-19] Analogously, mono- and bi-nuclear mixed-ligand copper(II) complexes containing the Schiff base b-[(3-formyl-5-methyl-2-hydroxy-benzylidene)amino]propionate ligand and 1,10'-phenanthroline or 4,4'-bipyridine were found to exert multiple anticancer functions by inhibiting cancer cell proliferation inducing apoptosis, and by suppressing angiogenesis.[20] *In vitro* studies showed that the antiangiogenic activity of the mononuclear complex could be related to a stabilization of G-quadruplex structures in the proximal VEGF promoter region determining a repression of the VEGF gene that, in turn, suppresses angiogenesis.[20] According to the authors, the binuclear complex, instead, exerts anticancer and antiangiogenesis activity mainly by inhibiting p-Akt and p-Erk1/2 activation.[21]

Based on these evidences, in the present study we report on the synthesis and characterization of two homoleptic, phosphino Cu(I) complexes $[Cu(DAPTA)_4]BF_4$ **2** and $[Cu(PTA\text{-}SO_2)_4]BF_4$ **3** containing 3,7-diacetyl-1,3,7-triaza-5-phosphabicyclo[3.3.1] nonane (DAPTA) and 2-thia-1,3,5-triaza-phosphoadamantane 2,2 dioxide ($PTA\text{-}SO_2$) as coordinating phosphines (Scheme 1).

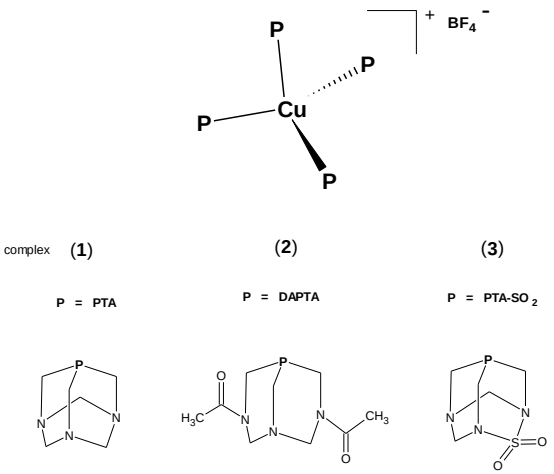

Scheme 1. Pictorial view of the ligands and complexes utilised in this study

Relevant structural information concerning the Cu site in $[Cu(DAPTA)_4]BF_4$ **2** has been obtained by X-ray Absorption Spectroscopy (XAS).[22-25] These novel Cu(I) complexes, together with the PTA derivative (PTA = 1,3,7-triaza-5-phosphabicyclo[3.3.1]nonane), $[Cu(PTA)_4][BF_4]$ **1**,[26] were tested for their cytotoxic properties against a panel of human cancer cell lines. Complexes **1-3** were also evaluated as potential antiangiogenic agents by monitoring their effects on migration and capillary-like tube formation of human umbilical vein endothelial cells (HUVEC) in comparison to the effects induced by the well-known antiangiogenic drug sunitinib. PTA and DAPTA complexes **1-2** induced a tumor-preferential cell growth inhibition over non-malignant cells, and displayed remarkable anti-angiogenic properties at concentrations that were not cytotoxic for HUVEC. *In vivo* studies were performed: *i)* in a model of solid tumour, the murine Lewis Lung Carcinoma-bearing (LLC) im injected in C57BL mice in order to evaluate the suppression of tumour growth and *ii)* in a Matrigel plug assay, as *in vivo* bioassay of physiological angiogenesis, to evaluate angiogenesis inhibition. For the first time it has been demonstrated that phosphino copper(I) complexes, beside a remarkable *in vivo* antitumor activity, are endowed with antiangiogenic properties.

Results and discussion

Synthesis and characterization of copper(I) complexes

Two PTA derivatives, namely DAPTA and $PTA\text{-}SO_2$ were utilized for the synthesis of new homoleptic, tetrahedral Cu(I) complexes (Scheme 1). DAPTA, analogously to the parent PTA phosphine, is highly water soluble (water solubility *ca.* 7.4 M), and has been extensively used in coordination chemistry.[27, 28] On the contrary, $PTA\text{-}SO_2$ is insoluble in water at room temperature, and only few examples of $PTA\text{-}SO_2$ complexes have been reported so far.[27, 28]

$[Cu(DAPTA)_4]BF_4$, **2** and $[Cu(PTA\text{-}SO_2)_4]BF_4$, **3** were prepared starting from the labile precursor $[Cu(CH_3CN)_4]BF_4$ by ligand exchange reactions using a 1:4 metal:ligand stoichiometric ratio in acetonitrile solution. Both complexes are white colored and air stable powders; **2** is soluble in water and acetonitrile, and **3** is soluble in DMSO, but sparingly soluble in water and in common organic solvents. Their identity has been assessed by elemental analysis (C, H, N), multinuclear NMR (^1H, ^{31}P, ^{13}C) and IR spectroscopies, and high resolution Electrospray Ionization Mass Spectrometry ESI-MS in the positive ion mode. Moreover, relevant structural information concerning the Cu site of complex $[Cu(DAPTA)_4]BF_4$, **2** was collected by X-ray absorption spectroscopy (XAS). Determination of the log P values via RP-HPLC methods[29] indicates that complex **2** is the most hydrophilic complex of the series (log P = - 0.59) followed by **1** (log P = 0.93) and **3** (log P = 2.75).

The infrared spectra of complexes **2-3** (Figures S1 and S5) showed the characteristic bands of the pertinent phosphine ligands: an intense C=O stretching vibration at 1636 cm^{-1} in complex **2**, and intense SO_2 stretching vibrations at 1377 and 1172 cm^{-1} in complex **3**, along with a broad band at *ca.* 1050 cm^{-1} due to the presence of the BF_4 counter anion in both complexes.

^1H NMR spectra of complex **2** collected in acetonitrile-d_3 or in dmso-d_6 showed a series of multiplets arising from diastereotopic methylene protons and two singlets due to unequivalent methyl protons. This pattern confirmed the magnetic unequivalence of methylene protons present in the DAPTA ligand itself.[30] As shown in Figure 1, methylene protons of DAPTA upper rim (a1, a2, b1 and b2) were the most affected upon copper coordination.

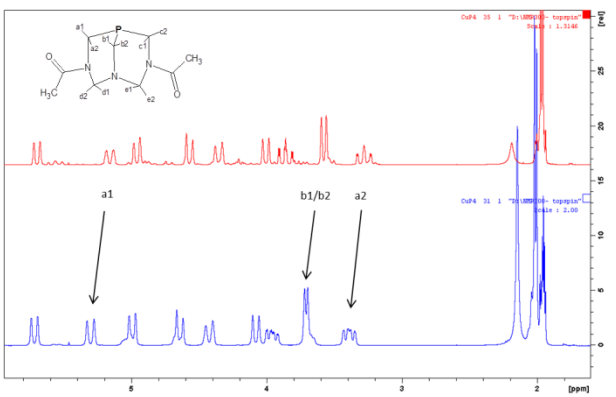

Fig. 1. ^1H NMR spectra of DAPTA (upper trace) and of $[Cu(DAPTA)_4][BF_4]$, **2** (lower trace) in acetonitrile-d_3. Numbering scheme of DAPTA ligand (insert).

The magnetic unequivalence of the acetyl groups was further validated by the presence of two quaternary acetylic carbons at 169.05 and 169.56 ppm and two methyl carbons at 21.20 and 21.75 ppm in the ^{13}C NMR spectrum (Figure S3). ^{31}P NMR of complex **2** showed a broad singlet centered at – 64.6 ppm (Figure S2), downfield shifted by 10.7 ppm compared to the corresponding signal in uncoordinated DAPTA. The lack of spherical symmetry in complex **2** precluded the observation of the characteristic quartet in the ^{31}P spectrum due to the ^{31}P-$^{63/65}Cu$ coupling, as observed in other spherical $[Cu(P)_4]^+$ complexes.[14, 20]

Analogously to what observed in complex **2**, ^{31}P NMR spectrum of complex **3** collected in DMSO-d_6 showed a broad singlet signal centered at δ = - 97.9, (Figure S7) downfield shifted with respect to the corresponding signal at δ = - 116.2 ppm shown by uncoordinated PTA-SO_2. In the ^1H NMR spectrum of complex **3** (Figure S6), the upper rim proton signals of coordinated PTA-SO_2 showed disappearance of the coupling with the P atom, as previously reported by other authors in PTA-SO_2 containing Au(I) and Pt(II) complexes.[31]
.

ESI(+)-MS spectrum of complex **2** recorded in methanol or acetonitrile solutions did not show the signal corresponding to the $[M]^+$ molecular ion, but only the fragment ions due to $[Cu(DAPTA)_2]^+$ and $[Cu(DAPTA)]^+$ at m/z 521 (100%) and 292 (20%), respectively (Figure S4). This behaviour is common for $[Cu(P)_4]^+$-type complexes, and the lack of the parent $[Cu(P)_4]^+$ ion was previously explained taking into account dissociation processes occurring in dilute solutions (*ca.* 10^{-5} M). [32, 33] Another low abundant ion at m/z 333 corresponding to the solvent adduct $[Cu(DAPTA)(MeCN)]^+$ was also observed in acetonitrile solution.

ESI(+)-MS spectra of complex **3** in DMSO showed only the peaks corresponding to the solvated species $[Cu(DMSO)_2]^+$ at m/z 219 and $[Cu(DMSO)]^+$ at m/z 141 (Figure S9); also acetonitrile solutions of complex **3** gave peaks corresponding to solvato species $[Cu(MeCN)_2]^+$ at m/z 145, and $[Cu(MeCN)]^+$ at m/z 104. No peaks corresponding to phosphine-containing adducts were detected. Instead, ESI(-)-MS spectra of complex **3** in acetonitrile solutions showed several peaks including both phosphine and the BF_4 counteranion. In detail, in the full ESI(-) spectrum peaks corresponding to $[Cu(PTA\text{-}SO_2)_2(BF_4)_2(MeCN)_2]^-$ (m/z 733), $[Cu(PTA\text{-}SO_2)_2(BF_4)_2]^-$ (m/z 651), $[Cu(PTA\text{-}SO_2)(BF_4)_2]^-$ (m/z 445), $[Cu(BF_4)_2]^-$ (m/z 237) and $[Cu(F)(BF_4)]^-$ (m/z 169) were detected (Figure S10). MS^n studies on the cluster ion $[Cu(PTA\text{-}SO_2)_2(BF_4)_2(MeCN)_2]^-$ at m/z 733 showed that it decomposed first through consecutive losses of PTA-SO_2 with formation of the fragment ions $[Cu(PTA\text{-}SO_2)(BF_4)_2(MeCN)_2]^-$ (m/z 526) and $[Cu(BF_4)_2(MeCN)_2]^-$ (m/z 319), followed by losses of BF_3 from the coordinated anion with formation of $[Cu(BF_4)(F)(MeCN)_2]^-$ (m/z 251) and $[CuF_2(MeCN)_2]^-$ (m/z 183). No further decomposition of the latter ion was detected confirming the presence of stable solvated ions, a behaviour already observed in the positive ion modality.

The difficulty of growing crystals of complexes **2** and **3** suitable for X-ray diffraction studies and the lack of unambiguous NMR and MS data confirming the $[Cu(P)_4]^+$ assembly prompted us to investigate the molecular structure at the Cu site in the representative $[Cu(DAPTA)_4]BF_4$, **2** by X-Ray Absorption spectroscopy (XAS). XANES spectra of Cu complexes displayed a typical feature in the rising part of the XAS spectrum which is assigned to the 1s-4p electronic transition.[34] Both position and intensity can be considered for local geometric purposes. Figure 2 panel (a) reports the normalized XANES spectra of the complex.
The observed position at 8983.4 eV falls among the values observed for Cu(I) complexes with similar environment.[22, 34] Also, the intensity value (normalized) of about 0.4 is typically observed in 4-fold coordinated Cu(I) complexes.[22, 35] A more qualitative structural information was obtained by the analysis of the extended x-ray absorption spectrum (EXAFS). According to XANES indications, we started the data analysis postulating a 'CuP_4' figure for the first atomic shell. While submitted, this choice was corroborated by a very recent study focused on the removal of copper from amyloid-b peptide using the PTA ligand as scavenger, that reported a similar XANES profile for the resulting $[Cu(PTA)_4]^+$ complex.[36]

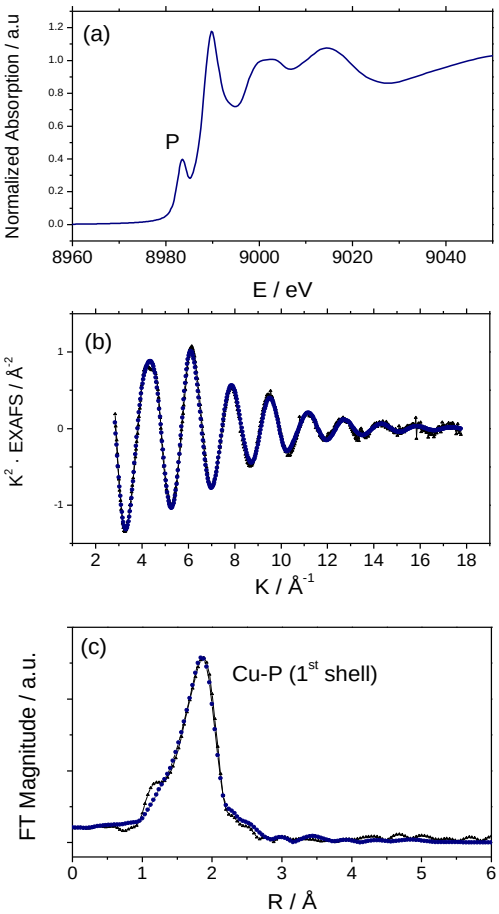

Fig. 2. XAS data for complex $[Cu(DAPTA)_4][BF_4]$, **2**. (a) Normalized XANES spectrum; (b) Best fit of the Cu K-edge EXAFS signal. The figure shows the comparison of the experimental (-) and theoretical (·) k^2-extracted EXAFS signals; (c) Comparison of the theoretical (·) and experimental (-) Fourier Transform signal relative to (b).

Details of such an analysis are available as Supporting Information. The outcome of the fitting procedure is illustrated in panels (b) and (c) of Figure 2 that contain the comparison of the k^2-extracted EXAFS signals (solid line) with the theoretical one (dotted line), and the corresponding Fourier Transform (FTs), respectively. Theoretical curves matched completely with the experimental ones in both panels confirming the 4-fold coordination of the Cu site in **2.** The best fit of the inter-atomic distance for the four equivalent Cu-P

Compound	IC_{50} (μM) ± SD									
	A549	A431	MCF-7	LoVo	A2780	HeLa	Capan-1	A375	HEK293	SI
$[Cu(PTA)_4][BF_4]$, 1	8.13±3.07	13.54±2.00	18.47±2.14	11.33±2.70	17.52±3.17	7.42±2.13	5.35±2.16	10.15±3.01	59.05±2.03	5.1
$[Cu(DAPTA)_4][BF_4]$, 2	18.16±2.13	12.25±3.13	17.15±2.16	8.25±3.17	25.27±2.86	21.24±2.29	9.52±1.96	19.35±1.25	79.95±1.35	4.8
$[Cu(PTASO_2)_4][BF_4]$, 3	21.14±2.14	18.64±1.25	19.25±2.15	12.52±3.13	21.97±2.44	23.45±2.87	13.23±3.41	23.23±3.03	73.24±3.16	3.8
PTA	>100	>100	>100	>100	>100	>100	>100	>100	>100	ND
$PTASO_2$	>100	61.12±4.36	69.46±3.35	>100	>100	>100	>100	>100	>100	ND
DAPTA	>100	>100	85.32±3.95	>100	>100	>100	>100	>100	>100	ND
cisplatin	12.64±0.81	2.25±0.21	7.60±0.21	8.53±1.14	3.64±1.03	10.50±1.51	9.81±1.38	1.29±2.11	19.56 ± 3.47	2.1

Table 1. Cytotoxicity assays. Cells (3-8 × 10^4·mL^{-1}) were treated for 72 h with increasing concentrations of tested compounds. Cytotoxicity was assessed by MTT test. IC_{50} values were calculated by a four parameter logistic model ($P < 0.05$). S.D.= standard deviation. ND: not determined

interactions is 2.256(2) Å with a corresponding EXAFS bond variance of 0.0057(3) $Å^2$ (see Table S1). This value is in perfect agreement with the Cu-P value of 2.258(2) Å obtained in the X-ray crystal structure determination of the similar complex $[Cu(PTA)_4][BF_4]·6H_2O$.[26, 37]

Cytotoxicity assays

The ability of complexes **1-3** and of the corresponding uncoordinated ligands (PTA, DAPTA and $PTA-SO_2$) to promote cell death was evaluated versus several human cancer cell lines derived from solid tumors (A549 lung, MCF-7 breast , LoVo colon, A2780 ovary, HeLa cervix, Capan-1 pancreatic adenocarcinoma cells and A375 melanoma cells) as well as versus HEK293 non-malignant fibroblasts. The cytotoxicity parameters, in terms of IC_{50} obtained after 72 h exposure by the MTT assay, are listed in Table 1. For comparison purposes, cytotoxicity of cisplatin was assessed under the same experimental conditions. Uncoordinated PTA, DAPTA and $PTA-SO_2$ ligands elicited a negligible cytotoxic activity (mean IC_{50} values over 90 μM). Complexes **1-3** showed a significant in vitro antitumor activity with IC_{50} values in the low micromolar range. Complex **1** emerged as the most cytotoxic derivative, eliciting mean IC_{50} values quite similar to those calculated for cisplatin (11.4 and 7.0 μM, respectively). Noteworthy, against human lung A549 and human pancreatic Capan-1 cancer cells complex **1** was roughly 2-fold more effective than cisplatin and overall, Capan-1 cancer cells were the most sensitive to the cell killing effect provoked by phosphino copper(I) complexes. Against non tumor cells in rapid proliferation (human embryonic kidney HEK293 cells), complex **2** was found the least cytotoxic (Table 1). Anyway, all copper(I) complexes elicited a cytotoxic activity lower than that recorded after cisplatin treatment; the selectivity index values (SI = quotient of the average IC_{50} toward non-malignant cells divided by the average IC_{50} for the malignant cells) calculated for complexes **1**, **2** and **3** were approximately 2 times higher than that calculated with the reference drug, attesting to a preferential cytotoxicity of copper(I) complexes versus neoplastic cells.

The antiproliferative effect of phosphino copper(I) complexes was also evaluated on HUVEC.

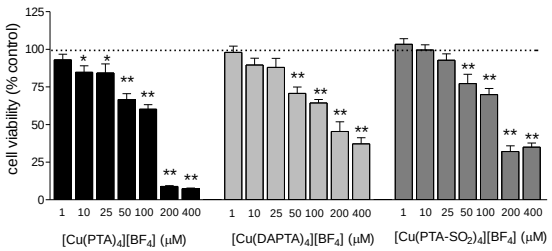

Fig. 3. Effect of copper(I) complexes on HUVEC viability and proliferation. HUVEC were treated for 48 h in complete culture medium in the presence of 1-400 μM of $[Cu(PTA)_4][BF_4]$, **1**, $[Cu(DAPTA)_4][BF_4]$, **2**, $[Cu(PTA-SO_2)_4][BF_4]$, **3**. Data are the mean ± SE of three independent experiments performed in quadruplicate (*P<0.05, **P<0.01 *vs* control cells, one-way ANOVA post test Dunnet).

As shown in Figure 3, treatment of exponentially growing HUVEC for 48 h with compounds **1**, **2** and **3** induced a moderate decrease of cell proliferation and viability with IC_{50} values of 119, 92 and 98 μM for compounds **1, 2** and **3**, respectively.

Effect of copper complexes on HUVEC migration

It is well-known that endothelial migration is a key process in angiogenesis. To determine whether compounds **1-3** could affect HUVEC migration the wound healing assay was performed. This in vitro test measures HUVEC haptotaxis (integrin-mediated non-directional motility) and is also advantageous as it allows long exposures of HUVEC to the tested compounds before performing the migration assay. The antiangiogenic potential of copper complexes was evaluated at concentrations that were not toxic for HUVEC (1-25 μM). As shown in Figure 4, pretreatment of HUVEC for 24 h with phosphino copper(I) complexes caused a concentration-dependent inhibition of wound closure respect to control cells and the relative inhibitory potency was: **1**>**2**>**3**. Treatment of HUVEC with the respective uncoordinated phosphine ligand (100 μM) did not affect HUVEC migration and wound closure (data not shown).

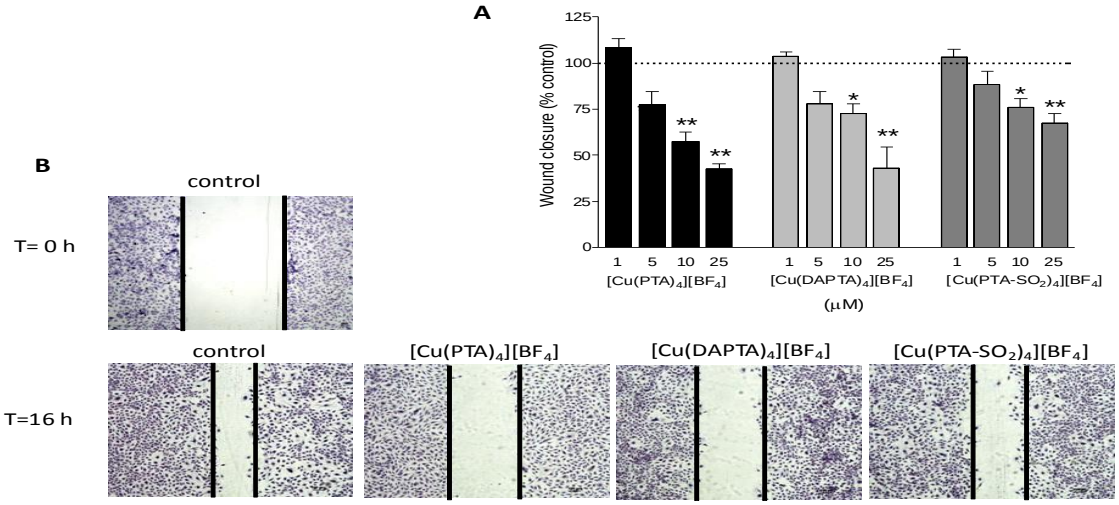

Fig. 4. Effect of copper(I) complexes on HUVEC migration. (A) Wound closure in HUVEC cultures after overnight incubation with 1-25 μM of $[Cu(PTA)_4][BF_4]$, **1**, $[Cu(DAPTA)_4][BF_4]$, **2**, $[Cu(PTA\text{-}SO_2)_4][BF_4]$, **3** in complete culture medium. Data are the mean ± SE of three independent experiments (*P<0.05, **P<0.01 *vs* control cells, one-way ANOVA post test Dunnett). (B) Phase contrast micrographs showing the effect of compounds **1**, **2** and **3** (25 μM) on HUVEC wound closure. Magnification x40.

Effect of copper complexes on capillary-like tube formation

Another important step in the angiogenic process is tubule formation. We investigated the ability of copper complexes to interfere with HUVEC differentiation into capillary-like tubes when seeded onto a suitable basement membrane matrix in the presence of an angiogenic stimulus. This assay is useful as an in vitro angiogenesis test since summarizes some fundamental steps of blood vessel formation, including endothelial cell adhesion, migration, alignment, protease secretion and tubule formation.[38] Figure 5A shows that control HUVEC placed on Matrigel formed robust, elongated tube-like structures after incubation with complete culture medium containing pro-angiogenic growth factors. After treatment with copper complexes (25 μM) a significant reduction of HUVEC tubularization occurred. Noteworthy, the effect induced by **1**-**3** was comparable to that shown by the clinically used antiangiogenic drug sunitinb (5 μM), a receptor tyrosine kinase inhibitor which targets VEGFRs and PDGFRs.[39] In figure 5B is depicted the effect of

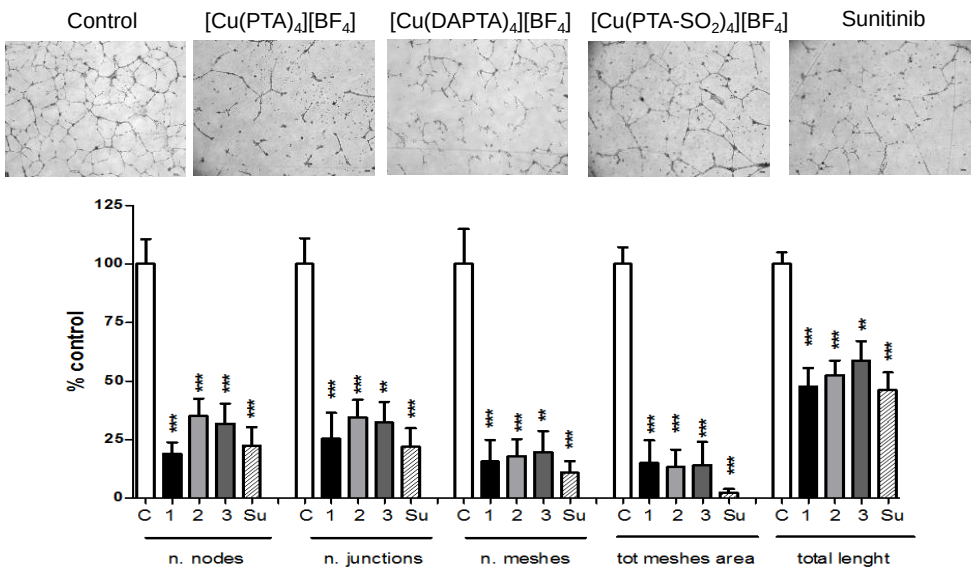

Fig. 5 Effect of copper(I) complexes on HUVEC ability to form capillary-like tubes. (A) Phase contrast micrographs showing the effect of 10 μM of $[Cu(PTA)_4][BF_4]$, **1**, $[Cu(DAPTA)_4][BF_4]$, **2**, $[Cu(PTA\text{-}SO_2)_4][BF_4]$, **3** and sunitinib (5 μM) on HUVEC tubularisation when cultured onto Matrigel™ for 16 h in complete cell culture medium. Magnification x40. (B) Quantitative analysis of the effect of compounds **1**, **2** and **3** (10 μM) and sunitinib (5 μM) on dimensional (total tubule length) and topological (number of nodes, junctions and meshes and total mesh area) parameters of the capillary-like network. Data are the mean ± SE of three independent experiments (**P<0.01, ***P<0.001 *vs* control cells, one-way ANOVA post test Bonferroni).

copper(I) complexes and sunitinib on dimensional (total tubule length) and topological parameters (number of nodes, junctions and meshes and total mesh area) of the capillary-like network. These results demonstrated that copper complexes **1**-**3** are able to hamper HUVEC tube formation.

In Vivo Antitumor Activity

Since from the in vitro studies complexes $[Cu(PTA)_4]BF_4$ **1** and $[Cu(DAPTA)_4]BF_4$ **2** distinguished themselves as the most promising derivatives, they were further evaluated for their potential antitumor effects in a model of solid tumor, the syngeneic murine Lewis lung carcinoma (LLC) implanted i.m. in C57BL mice. Copper complexes were firstly evaluated for their tolerability estimating the maximal-tolerated doses (MTD) for single intravenous (ip) dosing. MTDs calculated for **1** and **2** were about one order of magnitude higher than those recorded with cisplatin (data not shown). Copper complexes have been administered in aqueous solution taking advantage of their excellent solubility and stability in water. The tumour growth inhibition induced by treatment with copper complexes was compared with that promoted by the reference metallo-drug cisplatin tested using a standard protocol. Three days after tumor inoculation, tumor-bearing mice were randomized into vehicle control and treatment groups (7 mice per group). Control mice received the vehicle (0.9% NaCl), whereas treated groups received at day 3, 5, 7, 9, 11 and 13 after the tumor cell inoculum doses of **1** or **2** (50 $mg \cdot kg^{-1}$) or cisplatin (1.5 $mg \cdot kg^{-1}$). Tumor growth was estimated at day 15, and the results are summarized in Table 2. For the assessment of the adverse side effects, changes in the body weights of tumor-bearing mice were daily monitored (Figure 6). Chemotherapy with complexes **1** and **2** induced a marked reduction of tumor mass compared to the control group indicating that treatment of LLC-bearing mice with copper complexes leads to a tumor growth inhibition comparable to that achieved with cisplatin treatment. Noteworthy, the time course of body weight changes indicated that treatment with both copper complexes, mostly with complex **2** did not induce significant body weight loss and no signs of discomfort were evident, whereas mice treated with cisplatin appeared prostrate and showed substantial weight loss (Figure 6).

	Daily dose ($mg \cdot kg^{-1}$)	Average Tumor Weight (mean±S.D., g)	Inhibition of tumor growth (%)
control[a]	---	0.638±0.01	---
$[Cu(PTA)_4]BF_4$, 1	50	0.223±0.16**[b]	65.05
$[Cu(DAPTA)_4]BF_4$, 2	50	0.207±0.13**[b]	67.55
cisplatin	1.5	0.168±0.10**[b]	73.66

[a] vehicle (0.9% NaCl)[b] $^{**}p < 0.01$.

Table 2. *In Vivo* Anticancer Activity toward LLC. Starting from day 3 after tumor implantation, the tested compounds were administered intraperitoneally (ip) at day 3, 5, 7, 9, 11 and 13. At day 15, mice were sacrificed, and tumor growth was detected as described in the Experimental Section. The Tukey–Kramer test was performed.

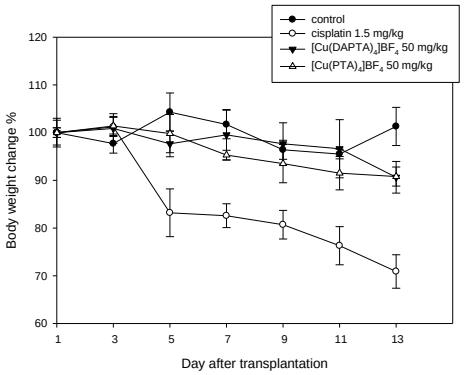

Fig. 6. Body weight changes. The body weight changes of LLC-bearing C57BL mice treated with vehicle or tested compounds. Each drug was administered at day 3, 5, 7, 9, 11 and 13 after the tumor cell inoculum. Weights were measured every two days. Error bars indicate the SD.

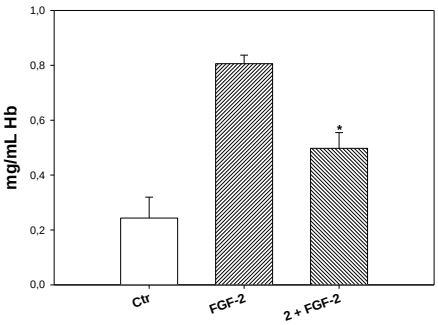

Fig. 7. Effects of $[Cu(DAPTA)_4][BF_4]$, **2** on in vivo angiogenesis. Quantitative haemoglobin (Hb) content in the Matrigel plug was determined using the Drabkin's Reagent kit. Bars are means ± S.D. of two separate experiments.

In Vivo Antiangiogenic Activity

The antiangiogenic potential of homoleptic copper(I) complexes was also investigated in vivo evaluating the neovascularization into a biocompatible polymer matrix containing a known angiogenic factor. Complex **2,** emerged as the most advantageous copper(I) complex, both in terms of antitumor efficacy and toxicity profile, was tested for its in vivo anti-angiogenic activity by means of an in vivo Matrigel plug assay as previously described.[40] As expected, the mean hemoglobin concentration in FGF-2-treated Matrigel plugs were much higher than that determined in control ones (Figure 7). Compound **2** significantly ($P < 0.05$) counteracted the FGF-2-induced neovascularization even if hemoglobin content was higher than the one of control plugs.

Experimental

Materials and General Methods.

The Cu(I) precursor $[Cu(CH_3CN)_4][BF_4]$ was prepared by reaction of $[Cu(H_2O)_6][BF_4]_2$ with metallic copper in acetonitrile. The ligands PTA,[41] DAPTA,[28, 30] and PTA-SO_2, [42] and the copper complex $[Cu(PTA)_4]BF_4$, **1** [26] were synthesized according to published methods. Elemental analyses were performed on a Carlo Erba 1106

Elemental Analyzer. ^{1}H, ^{31}P and ^{13}C NMR spectra were recorded on a Bruker AMX-300 instrument (300.13 MHz for ^{1}H, 75.47 MHz for ^{13}C and 121.41 MHz for ^{31}P), using $SiMe_4$ as internal reference (^{1}H and ^{13}C) and 85% aqueous H_3PO_4 as external reference (^{31}P). FT IR spectra were recorded on a Mattson 3030 Fourier transform spectrometer in the range 4000-400 cm^{-1} in KBr pellets. Mass spectra have been recorded by an electrospray LCQ ThermoFinnigan mass spectrometer. The purities of compounds **1-3** used for biological activity determination, were checked by elemental analysis and were found to be ≥95%.

Synthesis and Characterization of Homoleptic Phosphino Copper(I) Complexes.

A general procedure was employed for the synthesis of copper complexes **2** and **3**. To an acetonitrile solution (10 ml) of $[Cu(CH_3CN)_4][BF_4]$ (31 mg, 0.1 mmol) a stoichiometric amount of phosphine ligand (0.4 mmol) was added at room temperature. After 3 h the volume of the reaction mixture was reduced by solvent evaporation to *ca*. 2 mL. By addition of diethylether (4 mL) a white product was formed which was recovered by filtration and dried under vacuum.

$[Cu(DAPTA)_4]BF_4$ **(2)**

Yield: 82%. Anal. Calcd. for $CuBF_4C_{36}H_{64}N_{12}O_8P_4$: C 40.52, H 6.04, N 15.75. Found: C 40.37, H 6.07, N 15.68. IR (KBr, cm^{-1}): 1636s (C=O stretching), 1048s (BF_4 stretching). ^{1}H NMR (dmso-d_6) δ (ppm) = 5.59 (d, 1H, H^{e2}); 5.25 (d, 1H, H^{a1}); 4.98 (d, 1H, H^{d2}); 4.71 (d, 1H, H^{d1}); 4.40 (d, 1H, H^{c1}); 4.17 (d, 1H, H^{e1}); 4.05 (m, 1H, H^{c2}); 3.79 (m, 2H, $H^{b1\text{-}b2}$); 3.50 (d, 1H, H^{a2}); 2.02, 1.96 (2s, 6H, 2-CH_3). $^{31}P\{H\}$ NMR (CD_3CN): δ -60.1 (s, broad). $^{13}C\{H\}$ NMR (dmso-d_6): δ (ppm) = 169.62 (s, C^6-O); 169.20 (s, C^7-O); 66. 93 (s, N-C^5-N); 61.43 (s, N-C^4-N); 47.61 (s, P-C^2-N); 43.93 (s, P-C^3-N); 22.05 (s, C^8H_3); 21.61 (s, C^9H_3). ^{1}H NMR (CD_3CN) δ (ppm) = 5.73 (d, 1H, H^{e2}); 5.31 (d, 1H, H^{a1}); 5.01 (d, 1H, H^{d2}); 4.65 (d, 1H, H^{d1}); 4.44 (d, 1H, H^{c1}); 4.09 (d, 1H, H^{e1}); 3.99 (m, 1H, H^{c2}); 3.70 (d, 2H, $H^{b1\text{-}b2}$); 3.41 (m, 1H, H^{a2}); 2.01 (d, 6H, 2-CH_3). $^{31}P\{H\}$ NMR (CD_3CN): δ -64.6 (s, broad). $^{13}C\{H\}$ NMR (CD_3CN): δ (ppm) = 169.05 (s, C^6-O); 169.56 (s, C^7-O); 66. 90 (s, N-C^5-N); 61.34 (s, N-C^4-N); 46.99 (s, P-C^2-N); 43.08 (s, P-C^3-N); 37.75 (s, P-C^1-N); 21.75 (s, C^8H_3); 21.20 (s, C^9H_3). ^{1}H NMR (D_2O) δ (ppm) = 5.60 (d, 1H, H^{e2}); 5.51-4.86 (2H, H^{a1}, H^{d2}); 4.69 (1H, H^{d1}); 4.53 (d, 1H, H^{c1}); 4.22-4.12 (2H, H^{e1}, H^{c2}); 3.82 (m, 2H, $H^{b1\text{-}b2}$); 3.59 (m, 1H, H^{a2}); 2.04, 2.03 (2s, 6H, 2-CH_3). $^{31}P\{H\}$ NMR (CD_3CN): δ -59.2 (s, broad). ESI(+)MS in MeCN (*m/z* assignment, % intensity): 521 ($[Cu(DAPTA)_2]^+$, 30), 333 ([Cu + DAPTA + MeCN]$^+$, 5), 292 ($[Cu(DAPTA)]^+$, ≤ 5), 230 ([DAPTA + H]$^+$, 100). ESI(+)MS in DMSO/MeOH (*m/z* assignment, % intensity): 521 ($[Cu(DAPTA)_2]^+$, 45), 481 ([2DAPTA + Na]$^+$, 100), 252 ([DAPTA + Na]$^+$, 20). ESI(+)MS in H_2O/MeOH (*m/z* assignment, % intensity): 521 ($[Cu(DAPTA)_2]^+$, 40), 481 ([2 DAPTA + Na]$^+$, 100), 252 ([DAPTA + Na]$^+$, 40), 230 ([DAPTA + H]$^+$, 15).

$[Cu(PTA\text{-}SO_2)_4]BF_4$ **(3)**

Yield: 64%. Anal. Calcd for $CuP_4S_4O_8N_{12}H_{40}C_{20}BF_4{\cdot}CH_3CN$ C 25.90, H 4.25, N 17.85%. Found: C 26.09, H 4.41, N 17.75 %. IR (KBr, cm^{-1}) 1377s, 1172s (SO_2 stretching), 1051s (BF_4 stretching). ^{1}H NMR (dmso-d_6): δ (ppm) 4.00 (s, 2H, PC**H**$_2$N), 4.64 (AB quart,, 4H, PC**H**$_2$N), 5.01 (AB quart, 4H, NC**H**$_2$N) .^{31}P {H} NMR (dmso-d_6): δ(ppm) -97.9 (s, broad). $^{13}C\{H\}$ NMR (dmso-d_6): δ (ppm) 49.66 (bs, P**C**H$_2$N), 51.10 (bs, P**C**H$_2$N), 72.24 (bs, N**C**H$_2$N). ESI(+)-MS (*m/z* assignment, % intensity) in MeCN: 145 ($[Cu(MeCN)_2]^+$, 85), 104 ([CuMeCN]$^+$, 100); in DMSO/MeOH (219 $[Cu(DMSO)_2]^+$, 100). ESI(-)-MS (*m/z* assignment, % intensity) in MeCN: 733($[Cu(PTA\text{-}SO_2)_2(BF_4)_2(MeCN)_2]^-$, 45), 651 ($[Cu(PTA\text{-}SO_2)_2(BF_4)_2]^-$ 30), 444 ($[Cu(PTA\text{-}SO_2)(BF_4)_2]^-$ 70), 237 ($[Cu(BF_4)_2]^-$, 100), 169 $[Cu(F)(BF_4)]^-$, 40).

XAS data collection and data analysis

X-ray Absorption Spectroscopy experiments at the Cu K-edge were performed at the XAFS beamline of Elettra Synchrotron (Basovizza, Italy).[43] The storage ring operated at 2.0 GeV in top up mode with a typical current of 300 mA. The data were recorded at Cu K-edge in transmission mode using ionization chamber filled with a mixture of Ar and N_2 gas in order to have 20%, 80%, and 95% of absorbing in the I0, I1, I2 chambers, respectively. An internal reference of copper foil was used for energy calibration in each scan, allowing a continuous monitoring of the energy during consecutive scans. The energies were defined by assigning to 8980.3 eV the first inflection point of the spectrum of the metallic copper. The white beam was monochromatized using a fixed exit monochromator equipped with a pair of Si(111) crystals. Harmonics were rejected by using the cutoff of the reflectivity of the Platinum mirror placed at 3 mrad with respect to the beam upstream the monochromator and by detuning the second crystal (of the monochromator) by 30%. X-Ray absorption near edge structure (XANES) spectrum was normalized to an edge jump of unity. A prior removal of the background absorption was done by subtraction of a linear function extrapolated from the pre-edge region. The EXAFS spectrum was analyzed using the GNXAS package[44, 45] that takes into account the Multiple Scattering (MS) theory. The method allows the direct comparison of the raw experimental data with a model theoretical signal. Our initial structural model was based on the crystal structure (coordinates) of the DAPTA ligand.[28] More details on the XAS analysis are available as supplementary information.

Experiments with cultured human cells.

Cu(I) complexes 1 and 2, and the corresponding uncoordinated ligands and cisplatin were dissolved in 0.9% sodium chloride solution. Complex **3** was instead dissolved in the minimum amount of DMSO just before the experiment and a calculated amount of drug solution was added to the cell growth medium to a final solvent concentration of 0.5%, which had no detectable effect on cell killing. Endothelial cell growth supplement (ECGS), MTT (3-(4,5-dimethylthiazol-2-yl)-2,5-diphenyltetrazolium bromide) and cisplatin were obtained from Sigma Chemical Co, St. Louis, USA.

Cell cultures.

Human lung (A549), breast (MCF-7), cervical (HeLa), colon (LoVo), pancreatic (Capan-1) and ovarian (A2780) carcinoma cell lines along with melanoma (A375) cells were obtained by American Type Culture Collection (ATCC, RocKville, MD). Embryonic kidney HEK293 cells were obtained from European Collection of Cell Cultures (ECACC, Salisbury, UK). A431 are human cervical carcinoma cells kindly provided by Prof. F. Zunino (Division of Experimental Oncology B, Istituto Nazionale dei Tumori, Milan, Italy). Cell lines were maintained in the logarithmic phase at 37 °C in a 5% carbon dioxide atmosphere using the following culture media containing 10% foetal calf serum (Euroclone, Milan, Italy), antibiotics (50 units/mL penicillin and 50 µg/mL streptomycin) and 2mM l-glutamine: i) RPMI-1640 medium (Euroclone) for MCF-7, A431, A2780 and Capan-1 cells; ii) F-12 HAM'S (Sigma Chemical Co.) for LoVo, Hela and A549 cells; iii) DMEM for A375 and HEK293 cells. HUVEC were isolated as previously described[46] from human umbilical cords obtained after cesarean sections following informed consent from all the subjects. Cells were grown at 37°C under 5% CO_2 in medium M199 supplemented with 15% FBS, 100 µg/mL ECGS, 100 U/mL heparin, 2 mM L-glutamine, 100 U/mL penicillin-G, and 100 µg/mL streptomycin. HUVEC were used from passage 2 to 6.

MTT assay.

The growth inhibitory effect towards tumor cells was evaluated by means of MTT assay.[47] Briefly, 3–8 x 10^3 cells/well, dependent upon the growth characteristics of the cell line, were seeded in 96-well microplates in growth medium (100 µL). After 24 h, the medium was removed and replaced with a fresh one containing the compound to be studied at the appropriate concentration. Triplicate cultures were established for each treatment. After 48 (for HUVEC) or 72 h (for the other cell lines), each well was treated with 10 µL of a 5 mg/mL MTT saline solution, and following 5 h of incubation, 100 µL of a sodium dodecylsulfate (SDS) solution in HCl 0.01 M were added. After an overnight incubation, cell growth inhibition was detected by measuring the absorbance of each well at 570 nm using a Bio-Rad 680 microplate reader. Mean absorbance for each drug dose was expressed as a percentage of the control untreated well absorbance and plotted vs drug concentration. IC_{50} values, the drug concentrations that reduce the mean absorbance at 570 nm to 50% of those in the untreated control wells, were calculated by four parameter logistic (4-PL) model. Evaluation was based on means from at least four independent experiments.

Wound healing assay:

HUVEC (2 x 10^5 cells) were seeded in complete culture medium on 12-well culture plate and allowed to reach confluence. Subsequently, the media was replaced with complete medium containing the compounds tested. After 24 hours, one scratch was made and the media was replaced with fresh complete medium containing the drugs. Images were captured at 40X with a phase contrast inverted microscope (Nikon Eclipse Ti) equipped with a digital camera, immediately after the scratch was made (time 0) and after 16 hours of incubation. The wound spaces were measured from 10 random fields of view using ImageJ software. Quantitative analysis of cell migration was performed using an average wound space from those random fields of view, and the percentage of change in the wound space was calculated using the following formula: % change=(average space at time 0 h) - (average space at time 24 h)/(average space at time 0 h) × 100. Values were expressed as percent change from control cells.

Capillary–like tube formation assay

HUVEC (1×10^5 cells/well) were plated onto a thin layer (250 µL) of basement membrane matrix (Matrigel™, Becton Dickinson, Waltham, MA, USA) in 24-well plates. The cells were incubated at 37 °C for 16 h in complete cell culture medium with or without the tested compounds. Five images per well were captured at 40X with a phase contrast inverted microscope (Nikon Eclipse Ti) equipped with a digital camera. Images were analyzed using Angiogenesis Analyzer, a plugin developed for the ImageJ software.[48] Data on dimensional parameters (total tubule length) and topological parameters (number of nodes, junctions and meshes and total mesh area) of the capillary-like network were analyzed in control and treated wells. Values were expressed as percent change from control cells.

In vivo experiments

All experiments were performed according to D.L.G.S. 116/92 which warrants care of experimental animals in Italy. The research project was approved by the Italian Health Department according to the art. 7 of above mentioned D.L.

In Vivo Anticancer Activity toward Lewis lung carcinoma (LLC)

The mice were purchased from Charles River, Italy, housed in steel cages under controlled environmental conditions (constant temperature, humidity, and 12 h dark/light cycle), and alimented with commercial standard feed and tap water ad libitum. The LLC cell line was purchased from ECACC, United Kingdom. The LLC cell line was maintained in DMEM (Euroclone) supplemented with 10% heat-inactivated fetal bovine serum (Euroclone), 10 mM L-glutamine, 100 U mL^{-1} penicillin, and 100 µg mL^{-1} streptomycin in a 5% CO_2 air incubator at 37 °C. The LLC was implanted intramuscularly (i.m.) as a 2 × 10^6 cell inoculum into the right hind leg of 8 week old male and female C57BL mice (24 ± 3 g body weight). After 7 days from tumor implantation (tumor visible), mice were randomly randomized into vehicle control and treatment groups (7 mice per group) and treated at day 3, 5, 7, 9, 11 and 13 after the tumor cell inoculum with a i.p. injection of **1** and **2** (50 mg kg^{-1}), cisplatin (1.5 mg kg^{-1}) or the vehicle solution (0.9% NaCl). At day 15, animals were sacrificed by CO_2 inhalation, the legs were amputated at the proximal end of the femur, and the inhibition of tumor growth was determined according to the difference in weight of the tumor-bearing leg and the healthy leg of the animals expressed as a percentage referring to the control animals. Body weight was measured every 2 days and was taken as a parameter for systemic toxicity.

In Vivo Matrigel plug assay

Three-month-old C57/BL6 mice were anesthetized with isoflurane (2–3%) via nose cone and 100% oxygen used as carrier gas; the flank was shaved and disinfected with ethyl alcohol. A total of 0.5 mL of growth factor-reduced Matrigel (BD), mixed with 12 U.I. heparin (Vister) with or without 200 ng/plug FGF-2 and 10 µM compound 2, was injected subcutaneously into the right flank. After injection, the Matrigel polymerized forming a plug. After 7 days, the animals were sacrificed and the plugs were carefully removed and steeped in 300 µL/plug Brij-35 0.1% solution in PBS overnight at 4°C. Hemoglobin concentration was analyzed using Drabkin's Reagent kit (Sigma). The optical density was read at 540 nm using a Microplate autoreader EL 13. The results were expressed as mg/mL haemoglobin.

Statistical analyses

All of the values are the means ± SD of not less than three measurements starting from three different cell cultures. Multiple comparisons were made by ANOVA followed by Dunnett or Tukey–Kramer multiple comparison test (**P < 0.01; *P < 0.05), using GraphPad Software.

Conclusions

Three copper(I) phosphine complexes, whose $[Cu(P)_4]^+$ molecular structure has been assessed by XAS-EXAFS analysis, revealed a significant in vitro antiproliferative activity against several human cancer cell lines derived from solid tumors. Additionally, a tumor-preferential cell growth inhibition over non-malignant cells has been detected. In vitro monitoring of HUVEC migration and capillary-like tube formation evidenced an anti-angiogenic of copper complexes **1-3** at sub-cytotoxic concentrations. The dual in vitro cytotoxic and anti-angiogenic property has been corroborated by in vivo experiments in C57BL mice, on a murine model of solid tumor and on an established *in vivo* bioassay of physiological angiogenesis, respectively. Chemotherapy with complexes **1** and **2** induced a marked reduction of tumor mass without a significant body weight loss indicating that both complexes had smaller adverse side effects than cisplatin. Overall complex **2,** emerged as the most advantageous copper(I) complex, both in terms of antitumor efficacy and toxicity profile. Moreover, by the in vivo Matrigel plug assay the antiangiogenic properties of **2** have been confirmed.

Although combined antiproliferative and antiangiogenic effects promoted by copper complexes were previously reported in the literature,[20, 21] the biological basis for the sensitivity of angiogenesis to copper and the delineation of the cellular target(s) responsible of

the antitumor activity of copper-based agents remain elusive. In addition, it appears to be rather arduous (difficult) to match the above antiproliferative and antiangiogenic effects with the plethora of literature data concerning the pro-angiogenic activity of copper.[49] What is certain is that our phosphino Cu(I) complexes **1**-**3** are able to affect cancer cell viability and HUVEC migration/tubularisation at doses about 2 order of magnitude lower than that induced by copper ions.

Even if many aspects need to be elucidated, these findings have provided new insights for the development of tumor selective copper-based anticancer drugs.

Acknowledgements

This work was financially supported by the University of Padova (Progetto di Ateneo CPDA121973/12). M.G. is grateful to ELETTRA (Trieste, Italy) for the XAS measurements through the project #20115264. Authors thank Alessandro Orsetti for assistance in RP-HPLC analyses.

Notes and references

[a] Dipartimento di Scienze del Farmaco, Università di Padova, via Marzolo 5, 35131 Padova, Italy.

[b] IENI-CNR, Corso Stati Uniti 4, 35127 Padova, Italy

[c] Dipartimento di Chimica Industriale, Università di Bologna, Viale Risorgimento 4, 40136 Bologna, Italy

‡these authors contributed equally to the work

** Dipartimento di Scienze del Farmaco, Università di Padova, via Marzolo 5, 35131 Padova, Italy; Fax: +39 049 8275366; Tel: +39 049 8275347; e-mail: cristina.marzano@unipd.it

† Electronic supplementary information (ESI) available: ESI(-)-MS spectrum of complex **3** and XAS-EXAFS data of complex **2**.

1. C. Santini, M. Pellei, V. Gandin, M. Porchia, F. Tisato and C. Marzano, *Chemical Reviews*, 2014, 114, 815-862.
2. M. Diez, M. Arroyo, F. J. Cerdan, M. Munoz, M. A. Martin and J. L. Balibrea, *Oncology*, 1989, 46, 230-234.
3. K. Geraki, M. J. Farquharson and D. A. Bradley, *Physics in medicine and biology*, 2002, 47, 2327-2339.
4. S. B. Nayak, V. R. Bhat, D. Upadhyay and S. L. Udupa, *Indian J Physiol Pharmacol*, 2003, 47, 108-110.
5. H. Xie and Y. J. Kang, *Current Medicinal Chemistry*, 2009, 16, 1304-1314.
6. G. Narayanan, B. S. R, H. Vuyyuru, B. Muthuvel and S. Konerirajapuram Natrajan, *PLoS ONE*, 2013, 8, e71982.
7. J. Barralet, U. Gbureck, P. Habibovic, E. Vorndran, C. Gerard and C. J. Doillon, *Tissue Eng Part A*, 2009, 15, 1601-1609.
8. V. Antoniades, A. Sioga, E. M. Dietrich, S. Meditskou, L. Ekonomou and K. Antoniades, *Medical Hypotheses*, 2013, 81, 1159-1163.
9. L. Elsherif, Y. Jiang, J. T. Saari and Y. J. Kang, *Experimental Biology and Medicine*, 2004, 229, 616-622.
10. C. Marzano, V. Gandin, M. Pellei, D. Colavito, G. Papini, G. G. Lobbia, E. Del Giudice, M. Porchia, F. Tisato and C. Santini, *Journal of Medicinal Chemistry*, 2008, 51, 798-808.
11. S. Alidori, G. Gioia Lobbia, G. Papini, M. Pellei, M. Porchia, F. Refosco, F. Tisato, J. S. Lewis and C. Santini, *Journal of biological inorganic chemistry : JBIC : a publication of the Society of Biological Inorganic Chemistry*, 2008, 13, 307-315.
12. V. Gandin, M. Pellei, F. Tisato, M. Porchia, C. Santini and C. Marzano, *Journal of Cellular and Molecular Medicine*, 2012, 16, 142-151.
13. R. S. Kerbel, A. Viloria-Petit, G. Klement and J. Rak, *Eur J Cancer*, 2000, 36, 1248-1257.
14. G. Gasparini, R. Longo, M. Fanelli and B. A. Teicher, *Journal of clinical oncology : official journal of the American Society of Clinical Oncology*, 2005, 23, 1295-1311.
15. L. Wang, C. Zheng, Y. Liu, F. Le, F. Yang, X. Qin, C. Wang and J. Liu, *Biological Trace Element Research*, 2014, 157, 175-182.
16. T. Zou, C. T. Lum, C. N. Lok, W. P. To, K. H. Low and C. M. Che, *Angewandte Chemie*, 2014, 53, 5810-5814.
17. J. J. Zhang, R. W. Sun and C. M. Che, *Chemical Communications*, 2012, 48, 3388-3390.
18. R. W. Sun, M. F. Ng, E. L. Wong, J. Zhang, S. S. Chui, L. Shek, T. C. Lau and C. M. Che, *Dalton Transactions*, 2009, 10712-10716.
19. I. Ott, X. Qian, Y. Xu, D. H. Vlecken, I. J. Marques, D. Kubutat, J. Will, W. S. Sheldrick, P. Jesse, A. Prokop and C. P. Bagowski, *Journal of Medicinal Chemistry*, 2009, 52, 763-770.
20. X. Y. Qin, Y. N. Liu, Q. Q. Yu, L. C. Yang, Y. Liu, Y. H. Zhou and J. Liu, *Chemmedchem*, 2014, 9, 1665-1671.
21. X. Y. Qin, L. C. Yang, F. L. Le, Q. Q. Yu, D. D. Sun, Y. N. Liu and J. Liu, *Dalton Transactions*, 2013, 42, 14681-14684.
22. M. Giorgetti, L. Guadagnini, S. G. Fiddy, C. Santini and M. Pellei, *Polyhedron*, 2009, 28, 3600-3606.
23. M. Pellei, G. Papini, A. Trasatti, M. Giorgetti, D. Tonelli, M. Minicucci, C. Marzano, V. Gandin, G. Aquilanti, A. Dolmella and C. Santini, *Dalton Transactions*, 2011, 40, 9877-9888.
24. M. Giorgetti, S. Tonelli, A. Zanelli, G. Aquilanti, M. Pellei and C. Santini, *Polyhedron*, 2012, 48, 174-180.
25. M. Giorgetti, G. Aquilanti, M. Pellei and V. Gandin, *J Anal Atom Spectrom*, 2014, 29, 491-497.
26. M. Porchia, F. Benetollo, F. Refosco, F. Tisato, C. Marzano and V. Gandin, *Journal of Inorganic Biochemistry*, 2009, 103, 1644-1651.
27. J. Bravo, S. Bolano, L. Gonsalvi and M. Peruzzini, *Coordination Chemistry Reviews*, 2010, 254, 555-607.
28. D. J. Darensbourg, C. G. Ortiz and J. W. Kamplain, *Organometallics*, 2004, 23, 1747-1754.
29. A. V. Rudraraju, P. N. Amoyaw, T. J. Hubin and M. O. Khan, *Die Pharmazie*, 2014, 69, 655-662.
30. E. Vergara, S. Miranda, F. Mohr, E. Cerrada, E. R. T. Tiekink, P. Romero, A. Mendia and M. Laguna, *European Journal of Inorganic Chemistry*, 2007, 2926-2933.
31. M. Sternberg, C. H. Suresh and F. Mohr, *Organometallics*, 2010, 29, 3922-3929.
32. F. Tisato, F. Refosco, M. Porchia, M. Tegoni, V. Gandin, C. Marzano, M. Pellei, G. Papini, L. Lucato, R. Seraglia and P. Traldi, *Rapid Communications in Mass Spectrometry*, 2010, 24, 1610-1616.

33. F. Tisato, L. Crociani, M. Porchia, P. Di Bernardo, F. Endrizzi, C. Santini and R. Seraglia, *Rapid Communications in Mass Spectrometry*, 2013, 27, 2019-2027.
34. L.-S. Kau, Spira-Solomon, D. J.; Penner-Hahn, J. E.; Hodgson, K. O.; Solomon, E. I., *Journal of the American Chemical Society*, 1987, 109, 6433-6442.
35. I. J. Pickering, G. N. George, C. T. Dameron, B. Kurz, D. R. Winge and I. G. Dance, *Journal of the American Chemical Society*, 1993, 115, 9498-9505.
36. E. Atrian-Blasco, E. Cerrada, A. Conte-Daban, D. Testemale, P. Faller, M. Laguna and C. Hureau, *Metallomics: integrated biometal science*, 2015, DOI:10.1039/C5MT00077G.
37. A. M. Kirillov, P. Smolenski, M. F. C. G. da Silva and A. J. L. Pombeiro, *European Journal of Inorganic Chemistry*, 2007, 2686-2692.
38. D. A. Guidolin, G.; Ribatti, D.;, in *Microscopy: Science, Technology, Applications and Education*, ed. A. D. Méndez-Vilas, J., Formatex, Badajoz, Spain, 2010, vol. 2, pp. 876-884.
39. S. Faivre, G. Demetri, W. Sargent and E. Raymond, *Nat Rev Drug Discov*, 2007, 6, 734-745.
40. M. T. Conconi, G. Marzaro, A. Guiotto, L. Urbani, I. Zanusso, F. Tonus, M. Tommasini, P. P. Parnigotto and A. Chilin, *Invest New Drug*, 2012, 30, 594-603.
41. D. J. Daigle, *Inorganic Synthesis*, 1998, 32, 40-45.
42. A. B. P. J. D.J. Daigle, S.L. Vail, *J. Heterocycl. Chem.*, 1974 11, 407.
43. G. Aquilanti, M. Giorgetti, M. Minicucci, G. Papini, M. Pellei, M. Tegoni, A. Trasatti and C. Santini, *Dalton Transactions*, 2011, 40, 2764-2777.
44. A. Filipponi, *Journal of Physics-Condensed Matter*, 1995, 7, 9343-9356.
45. A. Filipponi, A. DiCicco and C. R. Natoli, *Physical Review B*, 1995, 52, 15122-15134.
46. M. C. Vinci, B. Visentin, F. Cusinato, G. B. Nardelli, L. Trevisi and S. Luciani, *Biochemical Pharmacology*, 2004, 67, 277-284.
47. M. C. Alley, D. A. Scudiero, A. Monks, M. L. Hursey, M. J. Czerwinski, D. L. Fine, B. J. Abbott, J. G. Mayo, R. H. Shoemaker and M. R. Boyd, *Cancer Research*, 1988, 48, 589-601.
48. G. M. Carpentier, M.; Courty, J.; Cascone, I.; Mondorf-les-Bains, Luxembourg, 2012.
49. L. Finney, S. Vogt, T. Fukai and D. Glesne, *Clinical and experimental pharmacology & physiology*, 2009, 36, 88-94.

